

## University of New Hampshire University of New Hampshire Scholars' Repository

---

Master's Theses and Capstones

Student Scholarship

---

Fall 2006

# A user-friendly system to measure electromyographic activity of dancers

Jianhua Zhou

*University of New Hampshire, Durham*

Follow this and additional works at: <https://scholars.unh.edu/thesis>

---

### Recommended Citation

Zhou, Jianhua, "A user-friendly system to measure electromyographic activity of dancers" (2006). *Master's Theses and Capstones*. 215.  
<https://scholars.unh.edu/thesis/215>

This Thesis is brought to you for free and open access by the Student Scholarship at University of New Hampshire Scholars' Repository. It has been accepted for inclusion in Master's Theses and Capstones by an authorized administrator of University of New Hampshire Scholars' Repository. For more information, please contact [nicole.hentz@unh.edu](mailto:nicole.hentz@unh.edu).

**A USER-FRIENDLY SYSTEM TO MEASURE ELECTROMYOGRAPHIC  
ACTIVITY OF DANCERS**

**BY**

**JIANHUA ZHOU**

**Bachelor of Science  
China University of Mining and Technology, 1996**

**THESIS**

**Submitted to the University of New Hampshire  
In Partial Fulfillment of  
the Requirements for the Degree of**

**Master of Science**

**in**

**Electrical Engineering**

**September, 2006**

UMI Number: 1437648

Copyright 2006 by  
Zhou, Jianhua

All rights reserved.

#### INFORMATION TO USERS

The quality of this reproduction is dependent upon the quality of the copy submitted. Broken or indistinct print, colored or poor quality illustrations and photographs, print bleed-through, substandard margins, and improper alignment can adversely affect reproduction.

In the unlikely event that the author did not send a complete manuscript and there are missing pages, these will be noted. Also, if unauthorized copyright material had to be removed, a note will indicate the deletion.

**UMI<sup>®</sup>**

---

UMI Microform 1437648

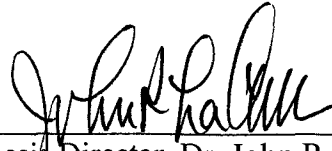
Copyright 2006 by ProQuest Information and Learning Company.

All rights reserved. This microform edition is protected against  
unauthorized copying under Title 17, United States Code.

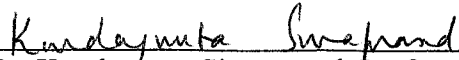
ProQuest Information and Learning Company  
300 North Zeeb Road  
P.O. Box 1346  
Ann Arbor, MI 48106-1346

ALL RIGHTS RESERVED  
2006  
Jianhua Zhou

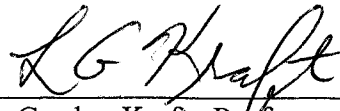
This thesis has been examined and approved.



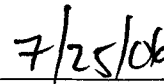
Thesis Director, Dr. John R. LaCourse,  
Chairman and Professor of Electrical  
and Computer Engineering



Dr. Kondagunta Sivaprasad, Professor of  
Electrical and Computer Engineering



Dr. Gordon Kraft, Professor of Electrical  
and Computer Engineering



Date

## **ACKNOWLEDGEMENTS**

I would like to thank Dr. John LaCourse for allowing me to work on this research under his supervision. His depth and width of knowledge, academic attitude and warm-hearted support impressed me and are greatly appreciated.

I would also like to express my thanks to Dr. Kondagunta Sivaprasad and Dr. Gordon Kraft for their support and constructive advice.

Additional thanks go to Wayne J. Smith, the PhD student of Dr. John LaCourse, who gave me valuable advice about my thesis.

Very special thanks are given to my husband Jeff Ju and my two cute sons David and Daniel, who offer me lots of happiness every minute.

## TABLE OF CONTENTS

ACKNOWLEDGEMENTS.....	iv
LIST OF FIGURES.....	vii
ABSTRACT.....	ix

CHAPTER	PAGE
I.INTRODUCTION AND BACKGROUND .....	1
II. SYSTEM DESIGN.....	4
1. Electrodes and Site Selection Strategies .....	5
2. Bio-Amplifier Design .....	8
2.1. Introduction.....	8
2.2 Instrumentation Amplifier.....	9
2.3 High-Pass Filter (HPF) and Low-Pass Filter (LPF) Implementation.....	12
2.4 Post amplification.....	16
2.5 Isolation Amplifier.....	18
3. A/D Conversion .....	20
3.1 Comparison of Solutions.....	20
3.2 USB-6009 Introduction and Challenges .....	20
4. Virtual Instrumentation Implementation.....	22
III.TEST AND RESULTS DATA.....	25
IV. SUMMARY.....	35
1. Future Work.....	36

LIST OF REFERENCES.....38



## LIST OF FIGURES

Figure 2.1 System Architecture Overview.....	4
Figure 2.2 Gastrocnemius Muscle.....	6
Figure 2.3 Electrode Positioning .....	7
Figure 2.4 Architecture of the Proposed Bio-Amplifier.....	9
Figure 2.5 Pre-amplifier (INA102) with Gain of 100.....	12
Figure 2.6 Circuit Schematic of HPF.....	14
Figure 2.7 Bode Plot of High Pass Filter.....	15
Figure 2.8 Schematic of Low Pass Filter (LPF).....	15
Figure 2.9 Bode Plot of Low Pass Filter.....	16
Figure 2.10 Post amplifier Schematics.....	17
Figure 2.11 Post Amplifier Gain Simulation.....	18
Figure 2.12 Architecture of Isolation Amplifier (ISO122).....	19
Figure 2.13 Analog Front End of USB 6009.....	20
Figure 2.14 Block Diagram to Show the Signal Flow in Virtual Instrumentation.....	22
Figure 3.1 Five Basic Ballet Positions for the Experiment.....	25
Figure 3.2 Jump Force Measurement of First Position.....	26
Figure 3.3a Jump Force Measurements for Position 2 in Figure 3.1.1.....	27
Figure 3.3b Jump Force Measurements for Position 2 with Muscles Half Stretched....	28
Figure 3.3c Jump Force Measurements for Position 2 with Take-Off Jump .....	29
Figure 3.4 Jump Force Measurement of Third Position in Figure 3.1.1.....	30
Figure 3.5 Jump Force Measurement of Fourth Position.....	31

Figure 3.6a Jump Force Measurements for Position 5 in Figure 3.1.1.....	32
Figure 3.6b Jump Force Measurements for Position 5 with Muscles Half Stretch.....	33
Figure 3.6c Jump Force Measurements for Position 5 with Take-Off Jump.....	34

## **ABSTRACT**

### **A USER-FRIENDLY SYSTEM TO MEASURE ELECTROMYOGRAPHIC ACTIVITY OF DANCERS**

by

Jianhua Zhou

University of New Hampshire, September, 2006

A data acquisition system aided by virtual instrumentation was developed to measure electromyographic activity of the dancers. The system is composed of three main components: 1) Analog front-end with signal conditioning, 2) USB serial interface based A/D conversion, and 3) virtual instrumentation designed in LabView tools. The proposed system is able to accurately collect the magnitude of jump force and displayed the data using virtual instruments with alarm functions. The signal path is well-conditioned and processed, which makes the device suitable for feasibility studies for future research.

## **CHAPTER I**

### **INTRODUCTION AND BACKGROUND**

The nature of dancing such as ballet movements is unusual, and therefore leads to some specific injuries. Knee pain, foot pain, and back pain, fractures, changing in bone density are a few of health problems that dancers experienced in their lives. Some injuries can be very serious and can affect dancers' career and living quality<sup>[1]</sup>.

Despite all the research that is done in order to prevent injuries in dancing, a large number of dancers still experience injuries of different severity and types. It is thought that one of the reasons for developing the injuries might be way they dance and train. The focus of this research is to develop a system to measure the electromyographic activity of the gastronemius muscle during work-out to measure the force while jumping. Interpretation of this data may aid in the prevention of injury.

Jumping is one of the skills that can create a great dancer. Jumping requires a combination of the right kind of muscle, tendon, foot shape and right ratio of body weight to strength. Roughly 15% of outcome of a jump comes from the ligaments in the arch of the foot which act as a spring. They flatten out as the knee bends, and spring back into shape as the dancer takes off into the air. About 35% of the jump comes from the tendons in the ankle and leg, particularly the Achilles tendon, which store potential energy as they

are stretched to prepare for the jump and release it explosively on take off. Tendons have more elastic potential than muscles, so the longer and thicker the tendon, the higher the jump. The lower leg of any sprinter or high jumper has a long Achilles tendon leading up to a high, ball-like calf muscle. The rest of the power in a jump, around 55%, is dependent on the muscle<sup>[2]</sup>.

To jump high, the dancer tries to increase the distance the center of gravity travels before take off. So the dancer bends his or her knees to jump. This puts the muscles, tendons and ligaments under tension, creating the potential for a reflex action which becomes the jump. It's like pulling an elastic band to its extreme before letting it snap. When you land from a jump, the force causes the tendons and muscles to stretch even further. Usually repeated jumps can cause injuries because of the overload jump force.

The research goal of this thesis is to design a user-friendly system to measure the electromyographic activity associated with jump force. The system can provide an alarm by determining the characterization of sEMG activity when the dancer's strain exceeds the allowable jump force. It is my hope that the system will teach the dancer to provide jump force optimally for conditioning and to avoid the situations that cause injury.

In this research, cascaded active filter design techniques have been used to construct the anti-alias filters for analog input signals before the A/D converter stages. LabView tools have been used to develop the virtual instrumentation (VI). Thus the system has the

conditioning. A full speed (12Mbps) Universal Serial Bus interface is used to bridge between PC and analog front end instrumentation.

capability to detect the signal of small magnitude by the amplification and well

In this thesis, four chapters are presented. Chapter I is the introduction of the research with the discussion to validate the thesis objective. Chapter II details the system design methodology for system implementation including hardware and virtual instrumentation designs. Data collected with the proposed instrumentation scheme is demonstrated in Chapter III under specific dance position. Finally the outlook for future potential work is outlined in Chapter IV.

## CHAPTER II

### SYSTEM DESIGN

The system includes four parts as shown in figure 2.1. The first stage is the electrodes which sense the signal from the muscle movement. The second stage involves mainly the hardware design (signal detecting and conditioning circuitry) while the third stage focuses on the analog signal processing and conversion to digital domain. The last stage is the virtual instrumentation to process the sampled data and generate the alarm through the LabView software tools.

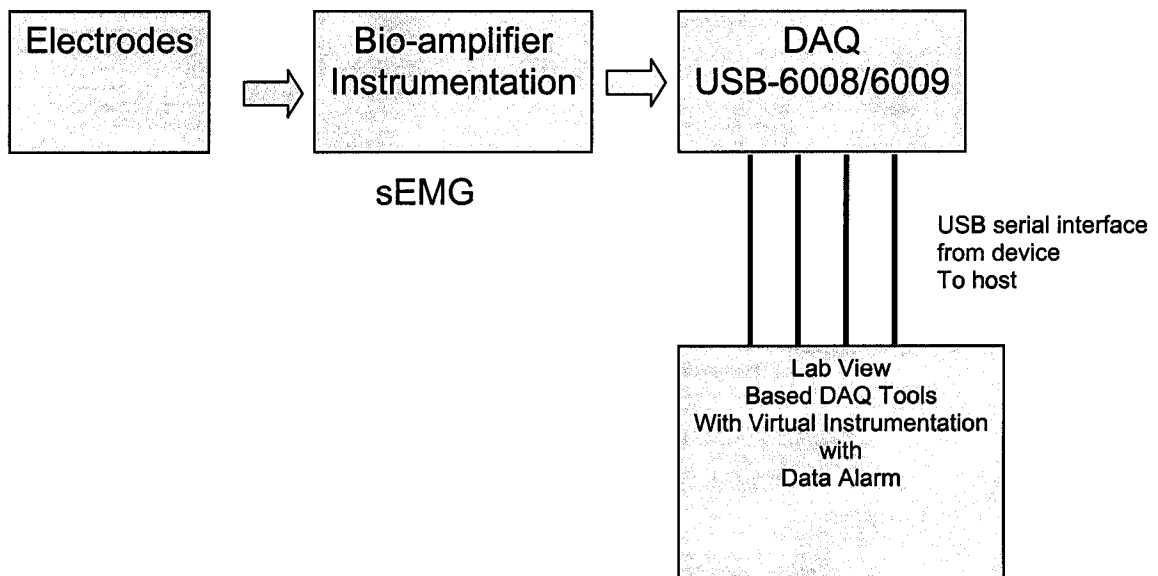


**Figure 2.1 System Architecture Overview**

## **1 Electrodes and Site Selection Strategies**

Before the whole system is addressed, it is necessary to understand the choice of electrodes and the site selection strategies. The sensors record the action potential from the muscle which crosses the electrode-skin interface. The lead-lok electrodes (F1010) were used in this experiment with a center snap having conductive liquid gel column. The size is about 1/16" (thick)  $\times$  1.75" (length)  $\times$  0.937" (width). Electrodes are like tiny microphones that are used to listen to muscles. Because there are several kinds of electrodes available on the market, the intended use of each type must be considered before selection of the electrode that provides the highest quality of surface electromyography (sEMG) recording.

To make the selection, one should consider the size of electrode. Electrodes with smaller detection areas allow closer inter-electrode spacing and thus a higher level of selectivity. For larger, broad muscle, electrodes with larger surface areas are desirable and may be placed farther apart. A common electrode on the market provides a 1-cm diameter pellet, placed an inter-electrode distance of 2 cm<sup>[3]</sup>. This size and spacing works for the application in this thesis.

One can measure the dancer's electromyographic activity by placing the electrodes on gastrocnemius (See figure 2.2). Because gastrocnemius crosses two joints, with the medial and lateral heads arising from just above the femoral condyles. Gastrocnemius also inserts into the calcaneus via the Achilles tendon (heel). The specific recordings from



the medial or lateral aspect may be obtained by placing electrodes 2 cm apart, just distal from the knee and 2 cm medial or lateral to midline<sup>[3]</sup> (see figure 2.3).

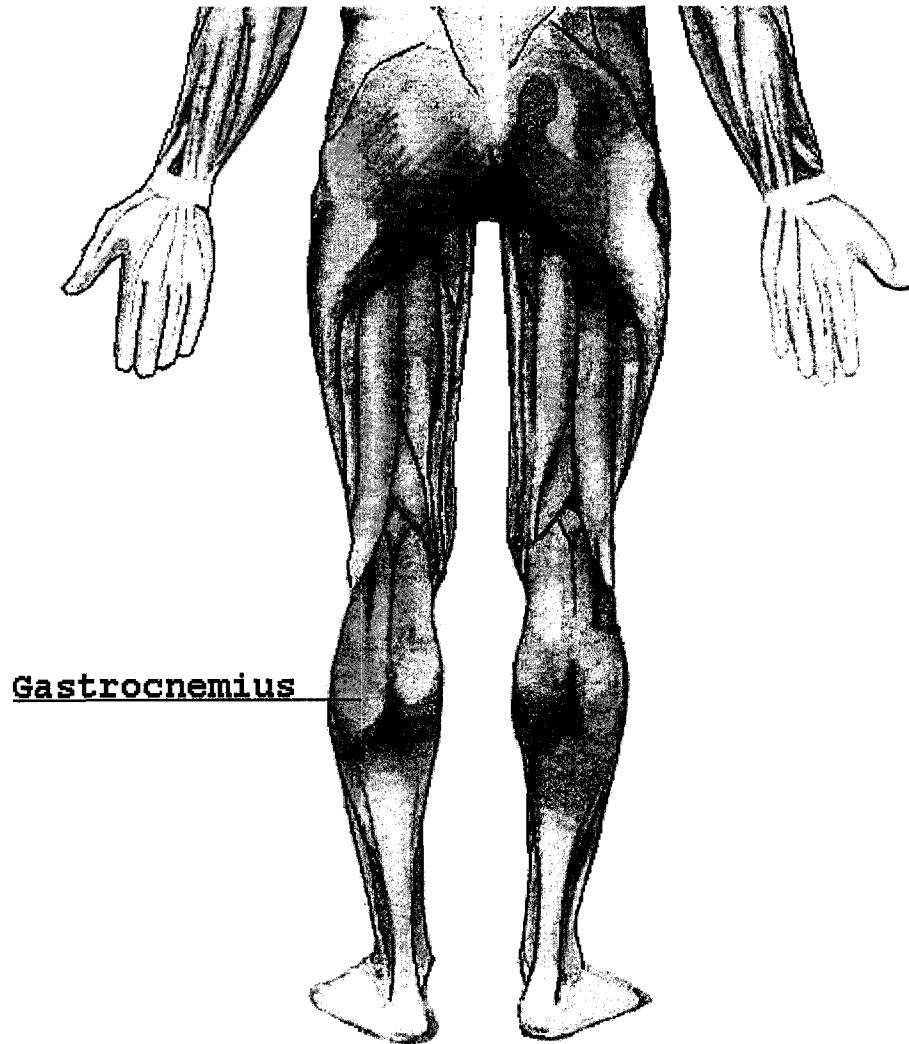


Figure2.2 Gastrocnemius Muscle

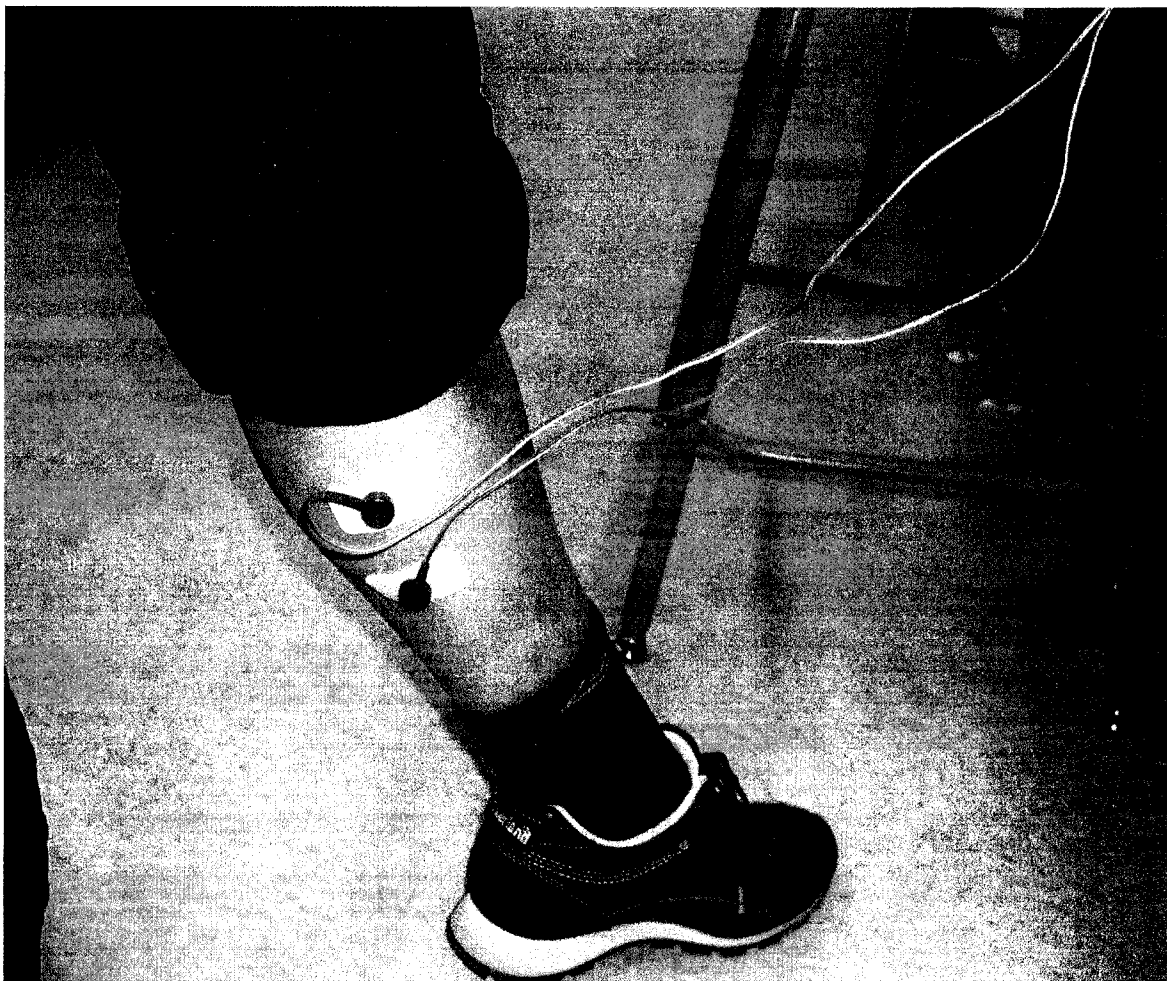


Figure 2.3 Electrode Positioning

## **2 Bio-Amplifier Instrumentation**

### **2.1 Introduction**

The energy that is generated by the muscle has a very small value and is measured in micro volts ( $\mu\text{V}$ ). It is necessary to use very sophisticated and sensitive instruments to amplify this signal so that it can be measured. In essence, a surface electromyography (sEMG) is a complex sensitive voltmeter.

Before one introduces why and how to design the bio-potential amplifier, let us discuss the source of the sEMG signal. It is the motor unit action potential (MUAP). Action potentials are generated by each of the motor units activated during a given contraction. In any given recruitment pattern, populations of motor units are activated in an asynchronous pattern. This asynchronous pattern of activation provides the possibility of smooth movement. The sum of the activity from all of the active motor units recruited for the given contraction can constitute the volume conducted signal, which is picked up at electrodes and amplified by the sEMG instrumentation.

The main stages of bio-potential amplifier are shown in Figure 2.4. They are the instrumentation preamplifier, the high-pass filter, the post amplifier, the isolation amplifier and the low-pass filter.

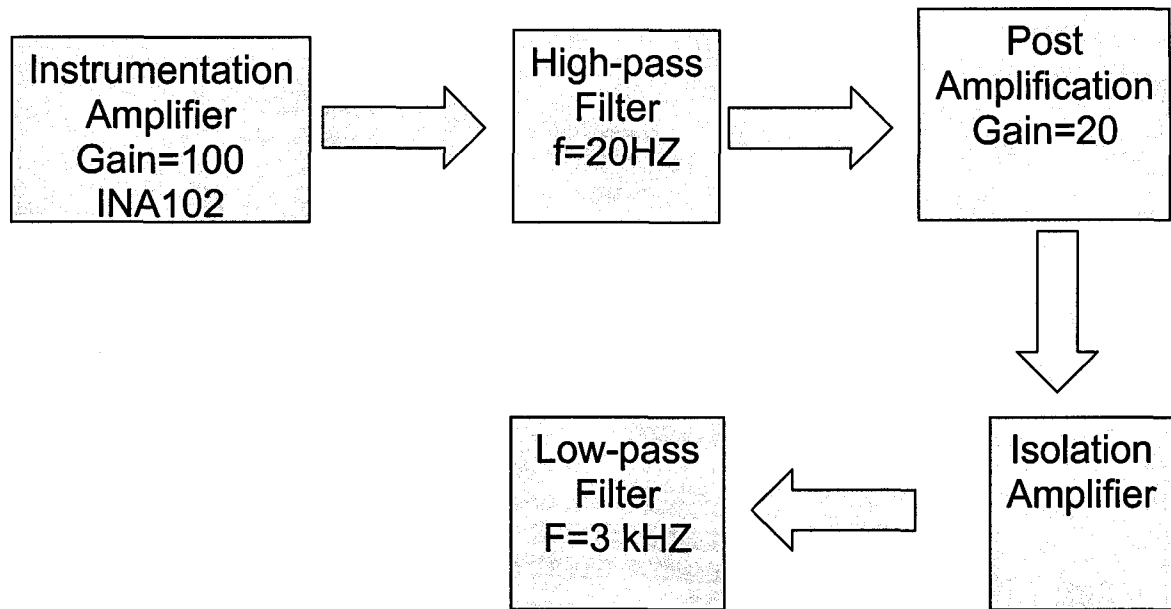


**Figure 2.4. Architecture of the Proposed Bio-Amplifier**

## 2.2 Instrumentation amplifier

Once the energy from the muscle reaches the skin, it is sensed by the electrodes. The interface between the sensing electrode and the skin is delicate matter. The impedance of the skin may vary as a function of the moisture of the skin; the superficial skin oil content; and the density of the dead-cell layer. In addition, some sort of electrolytic medium is commonly used to provide a cushion between the surface of the electrode and the surface of the skin. In sEMG, it is important to keep the impedance of the skin at the electrode site as low as possible and balanced for the two recording electrodes. This is commonly accomplished by abrading the skin vigorously with an alcohol pad. When the

impedance at the electrode skin interface is too high or too imbalanced, the common mode rejection of the sEMG amplifier is defeated.

How low should the impedance at the skin be to allow a valid and meaningful recording? The answer to this question depends upon the sEMG instrument. One attribute of the sEMG amplifier is its input impedance. The interface of skin impedance and input impedance must be matched in certain way. The input impedance of the pre-amplifier essentially absorbs the muscle energy that has reached the electrode-skin interface, and thus provides a basis for amplifying the small signal. Oscillating voltages can be measured only as a function of impedance. This is based on Ohm's law:  $E=IR$ . It is recommended that the impedance of the skin is less than that of the input impedance of the preamplifier. The input impedance of the sEMG preamplifier should be 10 to 100 times greater than the impedance at the electrode-skin interface. As a general rule, the greater the input impedance of the sEMG preamplifier, the better the measurement. This is because higher input impedance makes the sEMG more robust to poor electrode skin connections <sup>[3]</sup>.

After the action potential from the muscle has crossed the electrode-skin interface, it passes through the process of differential amplification and common mode rejection. During amplification, the size of biological signal is “boosted” or made larger. This is referred to as the gain. The amount of gain or amplification determines how large or how small the sEMG appears on the visual display.

Strong rejection of common –mode signal (noise) is one of the most important characteristics of a good bio-potential amplifier. This is accomplished with a high-quality instrumentation front-end amplifier. An instrumentation amplifier is a difference amplifier with a high common-mode reject ratio (CMRR) and high input impedance. The instrumentation amplifier used for this design is INA102 from Burr-Brown.

Why we use INA102 as the preamplifier of this system? The reason is as follows. The INA102 is a three--amplifier configuration which is used to provide the desirable characteristics of a premium performance instrumentation amplifier. In addition, it has features not normally found in integrated circuit instrumentation amplifiers. The input buffers incorporate high performance, low-drift amplifier circuitry. The amplifiers are connected in the non-inverting configuration to provide the high input impedance ( $10^{10} \Omega$ ) desirable in instrumentation amplifier applications. The output stage is connected in a unity-gain differential amplifier configuration. A critical part of this stage is the matching of the four  $20k\Omega$  resistors which provide the difference function. These resistors must be initially well matched and the matching must be maintained over temperature and time in order to retain good common-mode rejection. All of the internal resistors are made of thin-film nichrome on the integrated circuit. The critical resistors are laser-trimmed to provide the desired high-gain accuracy and common-mode rejection. Nichrome ensures long-term stability and provides excellent temperature coefficient of resistance (TCR) and TCR tracking. This provides gain accuracy and common-mode rejection when the INA102 is operated over wide temperature ranges.

In order to achieve the gain of 100 (The ratio between output voltage and the differential input voltage), pin3 to pin6 and pin7 needs to be shorted together based on the product data sheet requirement. The details are shown in figure 2.5.

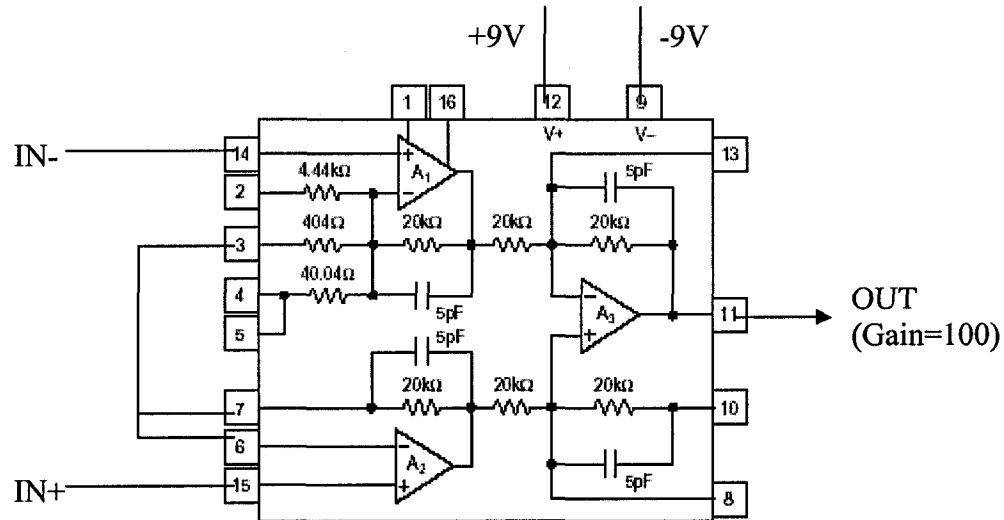


**Figure 2.5 Pre-amplifier (INA102) with Gain of 100**

### 2.3 High-Pass Filter (HPF) and Low-Pass Filter (LPF) Implementation

Once the sEMG signal has been boosted by the instrumentation amplifier, it is then processed by the high-pass filter and low-pass filter (band pass filter) stages. This filter passes only a certain frequency range of energy on for further quantification and display. Here a typical band pass filter might let all of the energy above 20Hz through and then block the signal above 3 KHz<sup>[6]</sup>. The lower cutoff point assists us by eliminating

much of the electrical noise associated with wire sway and miscellaneous biological artifacts associated with slow-moving DC potential shifts. The upper cutoff point eliminates the tissue noise at the electrode site and man made noise sources.

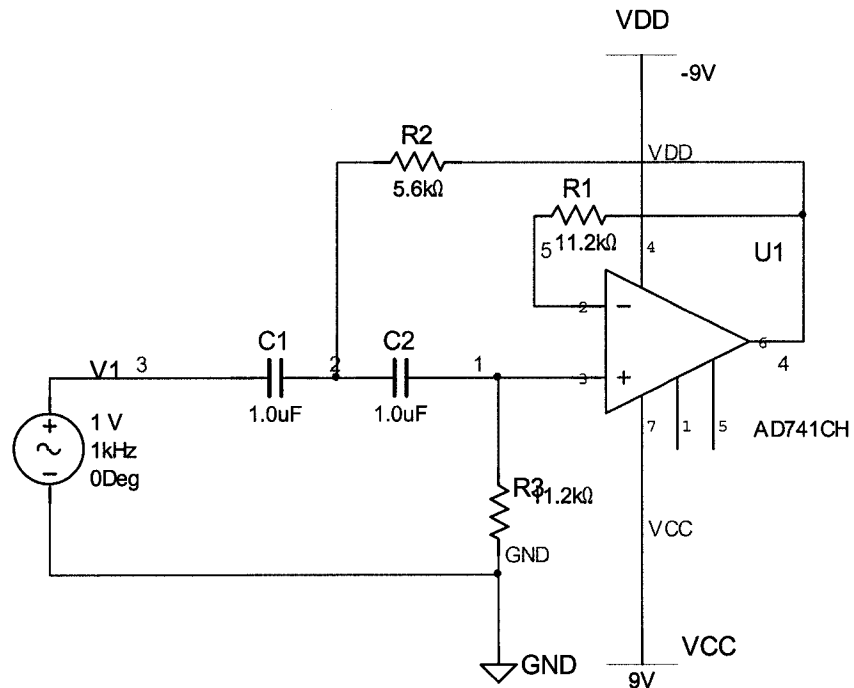
By using op amp and reactive elements, we can build active filters. Active filter have several advantages over passive filter. To begin with, we can eliminate the inductors, which are bulky and expensive at low cutoff frequencies. A mathematical analysis leads to the formula for the cutoff frequency:  $f_c = 0.707 / 2\pi R_2 C$  <sup>[5]</sup>. Normally we pick a common value for C, then we can calculate the value of R<sub>2</sub>.

Figure 2.6 shows the second-order high-pass filter. At low frequencies the capacitors appear open, and the voltage gain approaches 0. At high frequency, the capacitors appear shorted and the circuit becomes a voltage follower. Figure 2.7 illustrates the output response which is simulated in MUTISIM. Based on reference 6, 20Hz is the minimum frequency point for most electromyogram (EMG) signals and therefore the -3db bandwidth of this HPF was set to 20Hz.

Figure 2.8 shows the second-order low-pass filter. At low frequency region, both capacitors appear open, and the circuit becomes a voltage follower. As the frequency increases, the gain eventually starts to decrease until the frequency reaches -3 dB cutoff frequency. Figure 2.9 illustrates the bode plot (gain versus frequency) of this low pass



filter, which is simulated in MUTISIM. The value of 3 KHz is the -3db bandwidth set for this LPF again based on reference 6.



**Figure 2.6 Circuit Schematic of HPF**

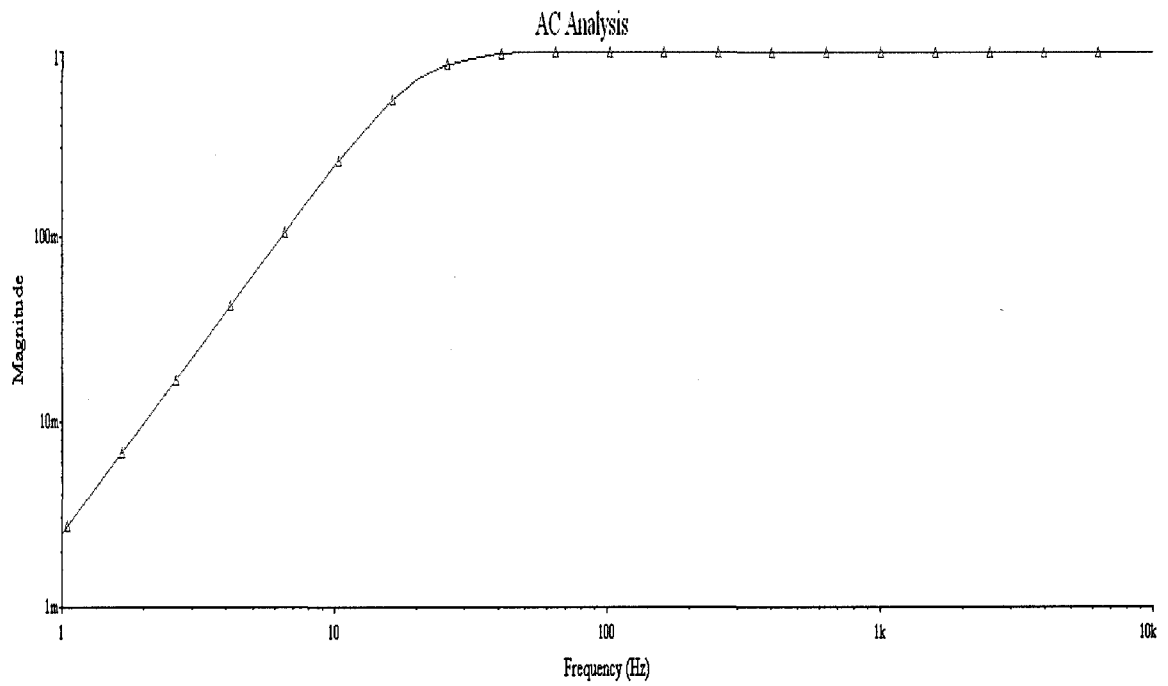


**Figure 2.7 Bode Plot of High Pass Filter**

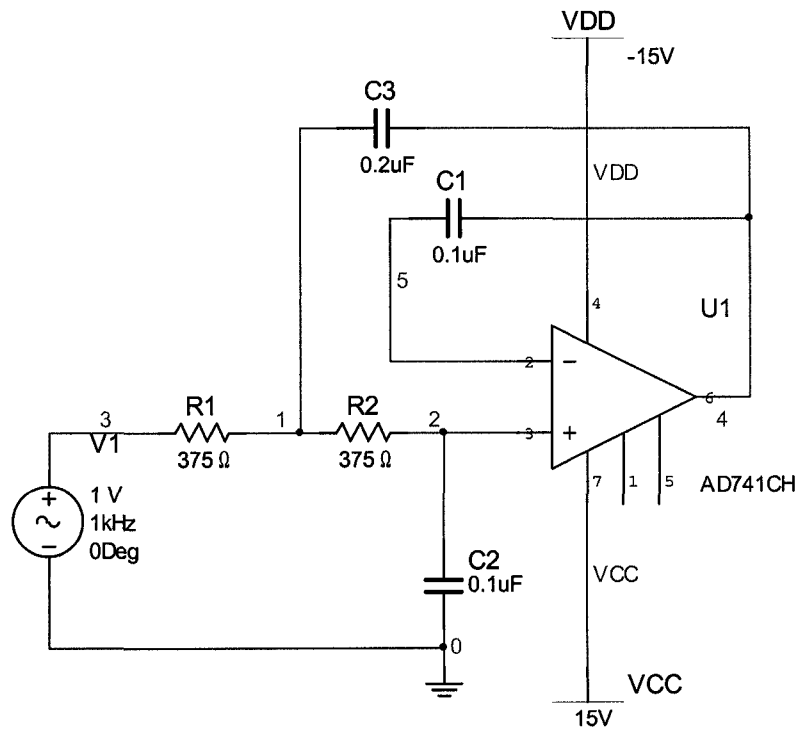


**Figure 2.8 Schematic of Low Pass Filter (LPF)**

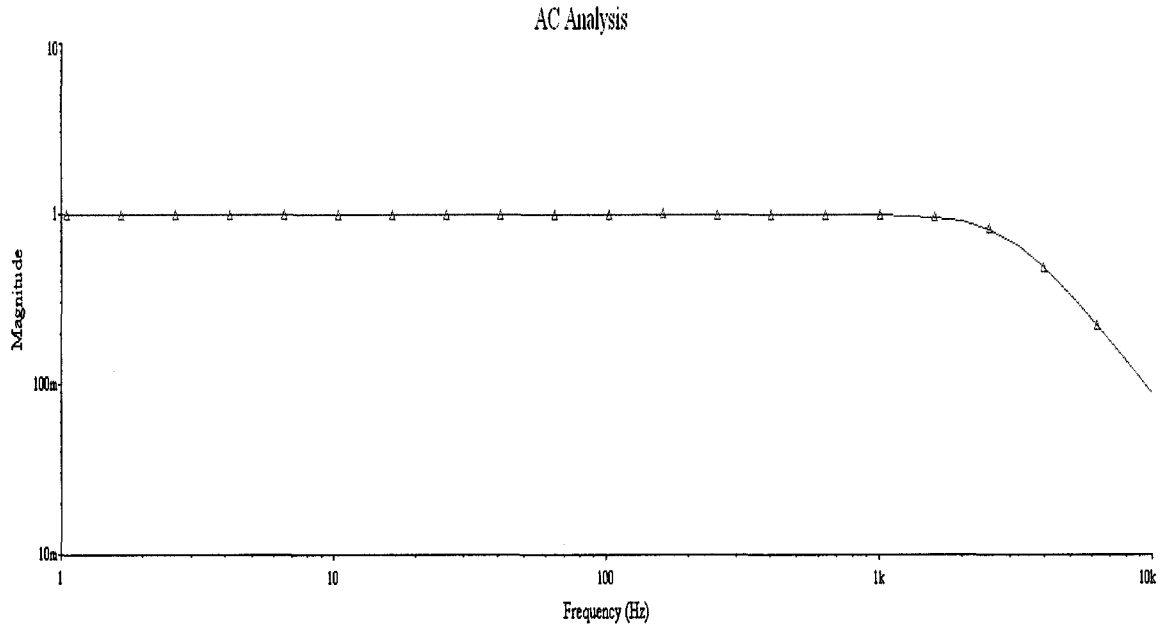


**Figure 2.9 Bode Plot of Low Pass Filter (LPF)**

## 2.4 Post Amplification

Normally the sEMG signal amplitudes are very small about 10  $\mu$ V-2mV. After they are boosted 100 times by instrumentation amplifier, the signal might be still very small in term of mini volts. Therefore, additional non-inverting amplifier in Figure 2.10 is added to further boost up the signal magnitude with the gain  $G = \left(1 + \frac{R_2}{R_1}\right)^{[5]}$ . By setting  $R_1 = 1K\Omega$  and  $R_2 = 19K\Omega$ , the gain is 20 (Figure 2.11). So now the signal amplitude can be boosted to several volts.

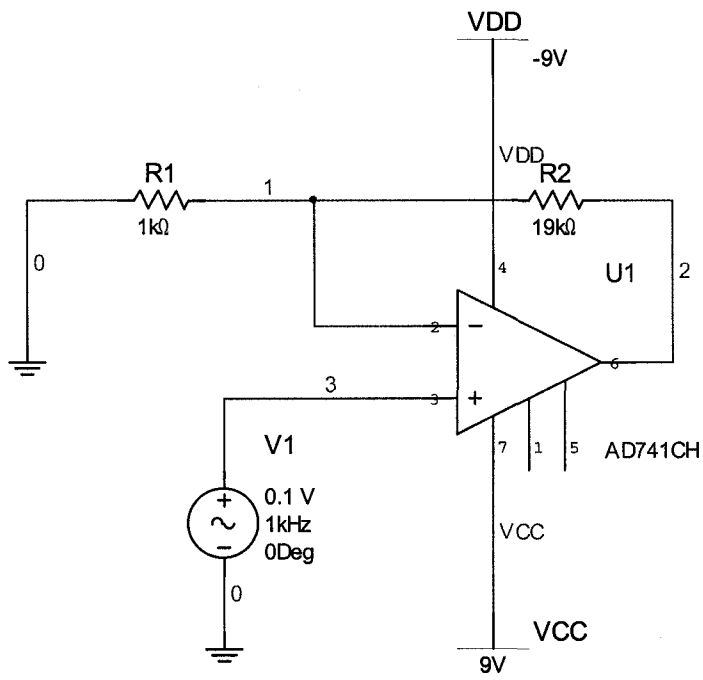


**Figure 2.10 Post amplifier Schematics**

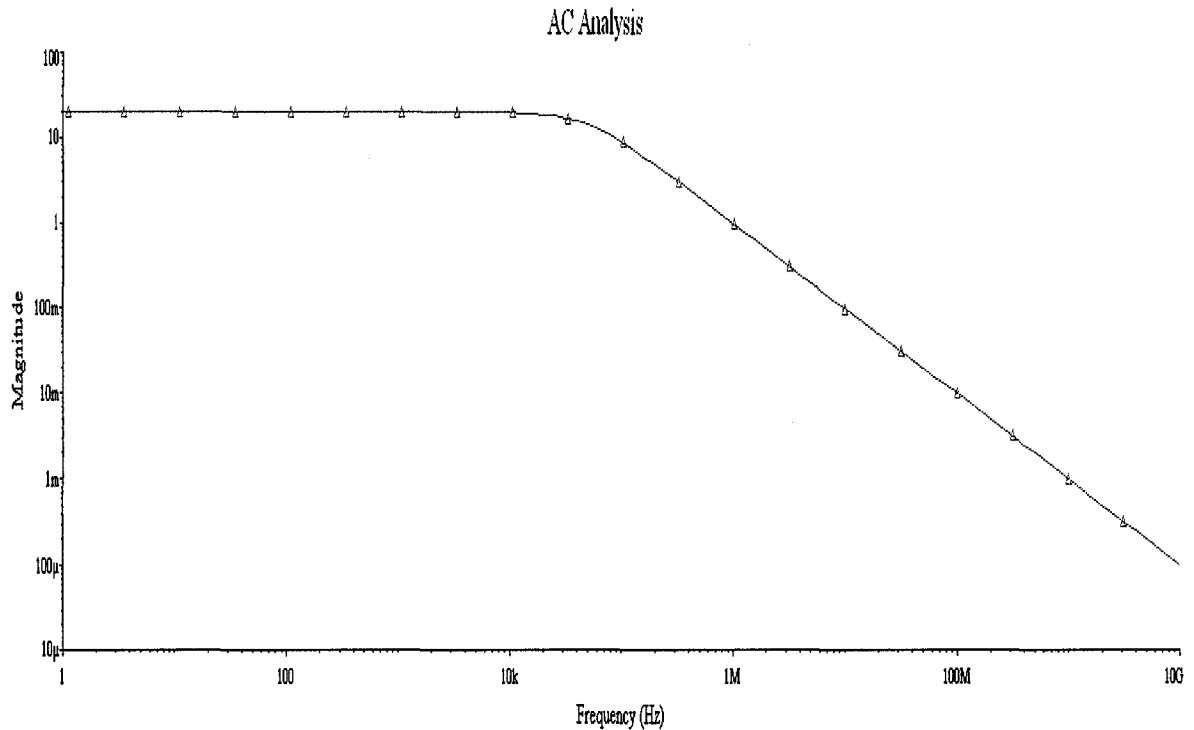


**Figure2.11 Post Amplifier Gain Simulation**

## 2.5 Isolation Amplifier

The system has to provide sufficient protection against electric shock to the user. Electric safety codes and standards specify the minimum safety requirements for the equipment. To that end, isolation amplifier can be used to break ground loops, to eliminate source-ground connection. Isolation amplification is realized in three different technologies: transformer isolation, capacitor isolation and opto-isolation. An isolation barrier provides a complete galvanic separation of the input side, i.e., the user and preamplifier, from all equipment on the output side. Ideally, there should be no flow of electric current across the barrier. An index is isolation-mode voltage, which is the voltage appearing across the

isolation barrier, i.e. between input common and output common. The isolation amplifier used for this design is the ISO122 from Burr-Brown.

The ISO122 isolation amplifier uses an input and an output section galvanically isolated by matched 1pF isolating capacitors built into the plastic package. The input is duty-cycle modulated and transmitted digitally across the barrier. The output section receives the modulated signal, converts it back to an analog voltage and removes the ripple component inherent in the demodulation. Input and output sections are fabricated, then laser trimmed for exceptional circuitry matching common to both input and output sections. The sections are then mounted on opposite ends of the package with the isolating capacitors mounted between the two sections. The detail structure is shown in figure 2.12.

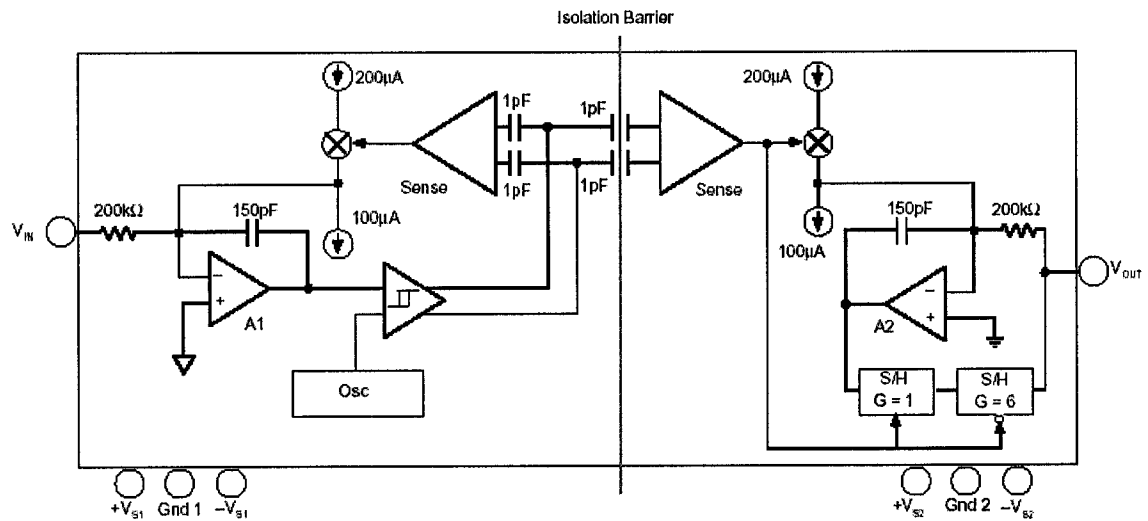


**Figure 2.12 Architecture of Isolation Amplifier (ISO122)**

### 3 A/D Conversion

#### 3.1 Solution Comparison

There are two major methods for the digital implementation for this system. One is micro-processor based implementation with A/D converter and micro-controllers. The major disadvantage of such implementation is the lack of virtual instrumentation capability. In order to visualize the dynamic transition of the jump force, USB interface based acquisition module offered by National Instrumentation is used for this design with capability to interface both analog and digital I/Os. The module is perfect for such applications with A/D converter integrated inside the module and the converted data are transferred to the PC or notebook via USB 1.1 full speed USB serial interfaces (12Mbps), which is much faster than traditional micro-processor based design with the UART interface (19.2Kbps for typical PC 8250 UART).

#### 3.2 USB 6009 introduction and challenges

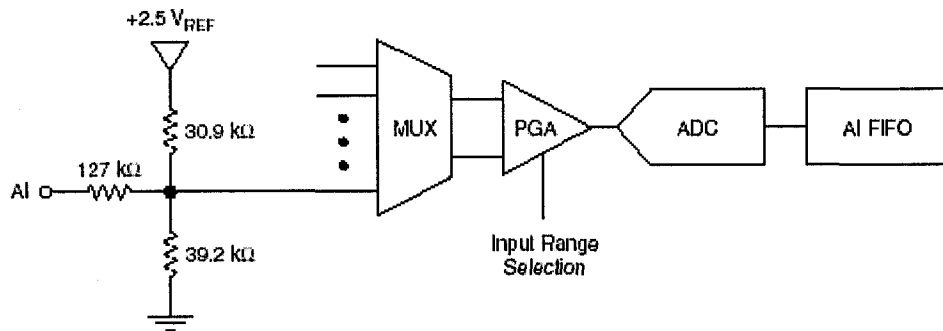


**Figure 2.13 Analog Front End of USB 6009**

Based on the users' guide of USB6009, the analog front end is shown as the figure 2.13. First the input can be configured by software named NI-DAQmx Base Task Configuration Utility for either differential input or single ended. Without the presence of signal input, the input is biased at 1.4V DC due to the internal clamp. It can be also observed, the input signal is scaled by 8.33: 1, which means 10V input will be scaled to 1.2V to fit the dynamic range of A/D converter operating under 2.5V.

$$SF_{input\_E} = \frac{R_{TH}}{R_{TH} + R_{IN}} = \frac{39.2K // 30.9K}{(39.2K // 30.9K) + 127K} = 0.12$$

Where the  $SF_{input\_E}$  is the scaling factor for A/D converter inside the USB 6009 module.  $R_{TH}$  is the Thevenin equivalent resistance looking into the A/D converter at the input node. In addition to the dynamic range complexity of the analog input signals, the sampling rate choice is also a challenging one. Analog signal from front end is processed by USB6009 hardware performing A/D conversion. The A/D converter output is fed into the computers via USB 1.1 signaling technology. The input signal scanning rate is defined in the NI-DAQmx Base Task Configuration Utility. For example, the sampling rate is 10 KHz, which means that the time interval between two continuous samples is 0.1 ms. Considering that the highest frequency in the incoming signal is smaller than 3 KHz, sampling frequency of 10 KHz (greater than twice of the signal bandwidth) is chosen based on Shannon sampling theorem.

If we choose from front panel with 1000 samples to display, which means the display window will refresh every 100ms. The sampling process keeps running by “WHILE”



loop. “WHILE” loop is controlled by the error in the arithmetic or “STOP” button on the front panel.

#### 4 Virtual Instrumentation Implementations

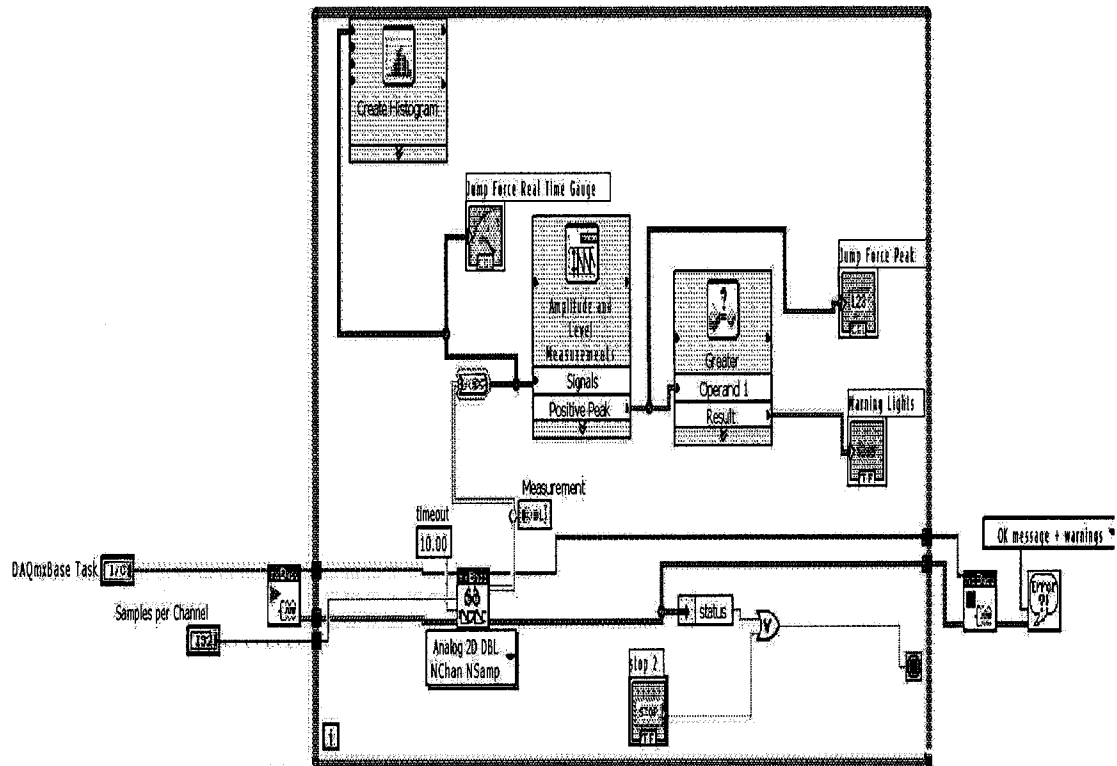


**Figure 2.14 Block Diagram to Show the Signal Flow in Virtual Instrumentation**

In order to design the virtual instrumentation using LabView, two steps need to be done. Firstly, you need to define the front panel display such as Waveform, Alarm LED and Real time gauge. The human-to-machine interface needs to be defined so that the user can enter the number of samples to be displayed. All the work is done through the front panel design. Please refer to the data section in Chapter 3 to see the format of the front panel. Secondly, the scheme to drive the display needs to be designed. All the schemes

behind to drive the data flow of the display module such as LED and Gauge are implemented in term of block diagrams, another toolbox of LabView to allow users to design the signal processing algorithm.

Figure 2.14 is the block diagram behind the front panel to sample the coming data from USB-6009 module. The data is analyzed with the real time monitoring and alarm system. The task is configured in NI-DAQmx Base Task Configuration Utility. The task defined include the signal property (single ended in this research), the monitored channel (channel 0 used in this design), sampling frequency (10KHz in this design) and the voltage scale (-10V min to 10V max in this design).

After the definition of the task and the samples quantity to be displayed in virtual scope, the engine begins to receive the sampled data and displayed by the “measurement” function icon in figure 2.14. “Measurement” is one of functional tools (Waveform Graph) in Controls Palette Toolbox. In the same time, dynamic data is fed into the “Amplitude and Level Measurement” function ( Analysis Tools of Function Palette). The peak positive value property is defined for this measurement to monitor the maximum value of the incoming signal. When the peak value is higher than the alarm threshold (2V is used as alarm point for trial but it is configurable in software) set inside the comparator, system will turn ON the LED lights on the front panel. LED warning lights will be turned ON from GREEN to RED with characters changing from “OFF” to “ON” whenever the alarm function is activated. In addition, on the front panel, a real time gauge is used to

display the data from jump force measurement. A peak value indicator is used to display the peak value for incoming samples.

## CHAPTER III

### TEST AND RESULT DATA

In this chapter, a total 5 positions of basic ballet positions are described and measured with the proposed system implementation above. The author was the volunteer in this research. Figure 3.1 is the diagram for those positions. The data collected in this experiment is based on these positions in either still standing, half strained or full jump. Limited by the availability of professional ballet performer, the acquisition data may not truly reflect the actual data of a professional performer's muscle movement.

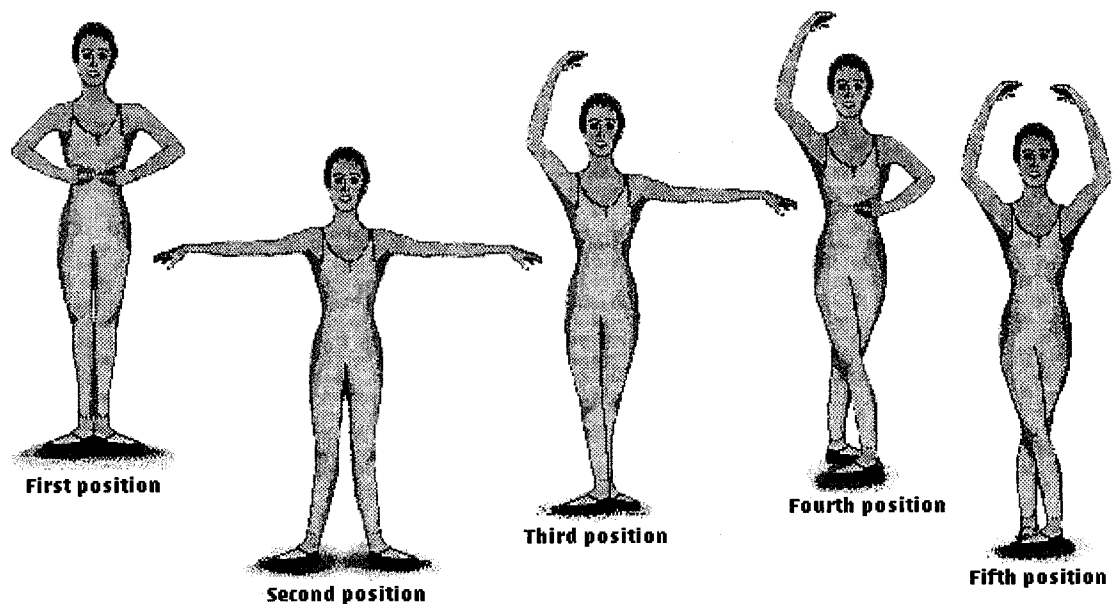


**Figure 3.1 Five Basic Ballet Positions for the Experiment**

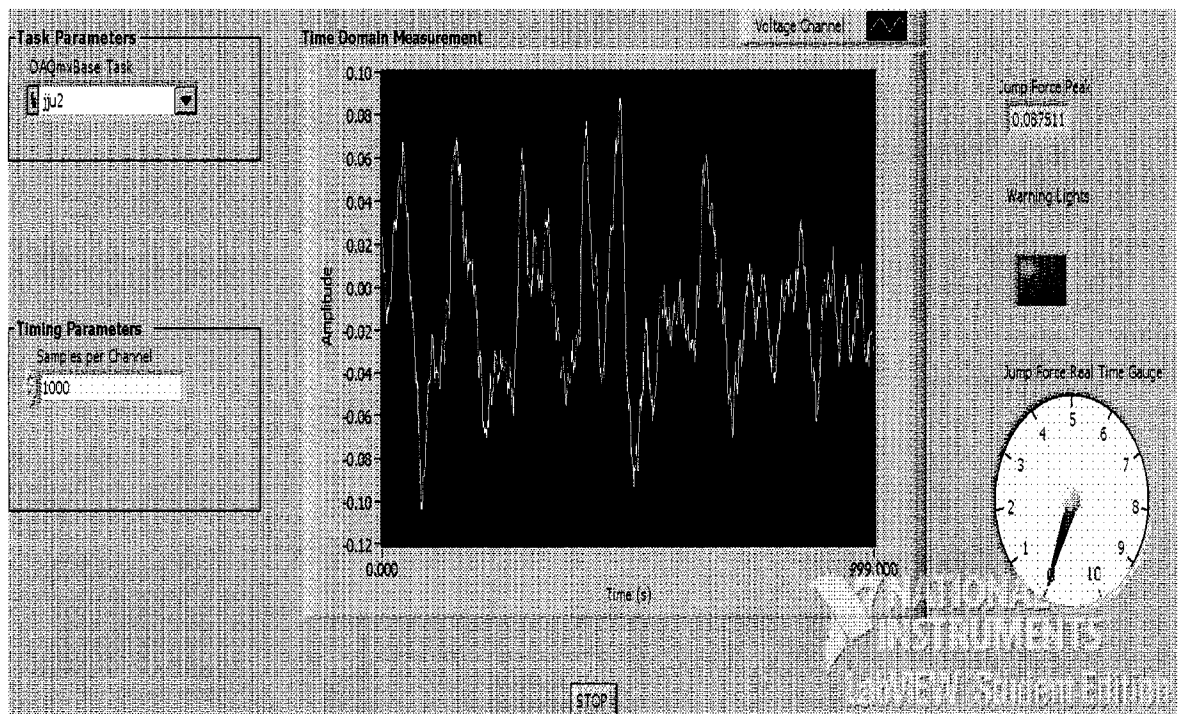
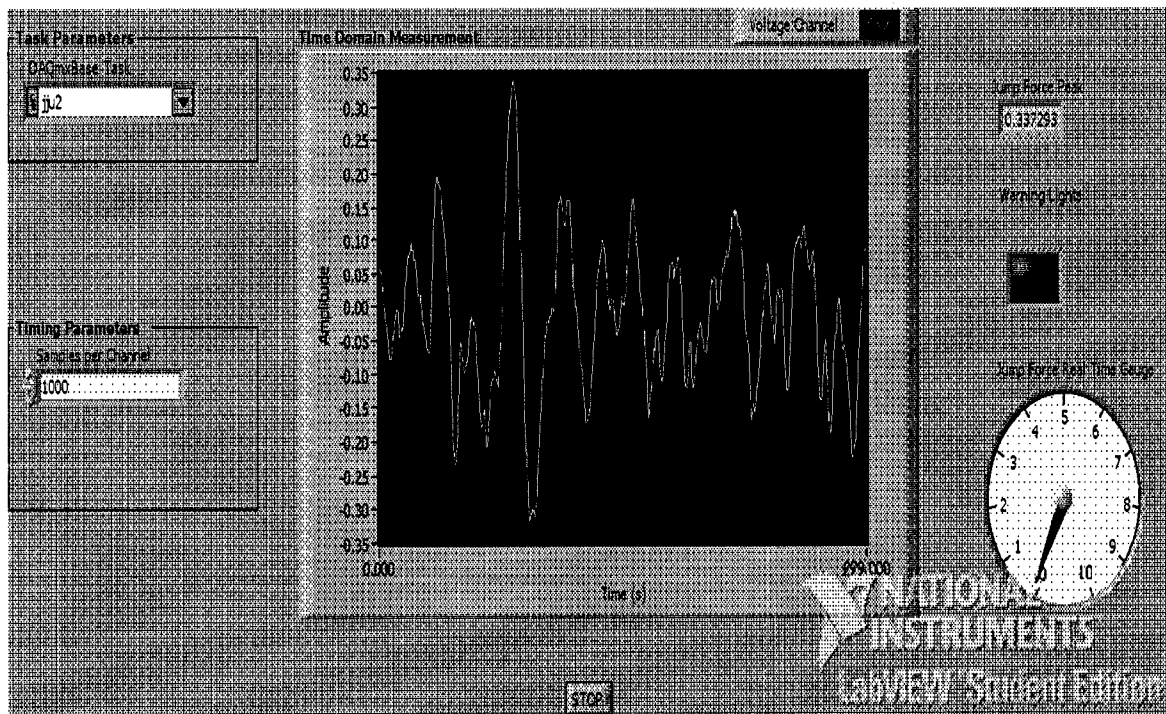


**Figure 3.2 Jump Force Measurement of First Position**

Figure 3.2 is the jump force measurement of the position 1. It has the peak (maximum of measured jump force) of about 67mV and the alarm LED is at OFF position. The alarm threshold is programmable. For this particular experiment, 2V is set for experiment only. End users can set the desirable value based on the statistic analysis. The gauge is used to dynamically display the jump force via the virtual instrumentation.

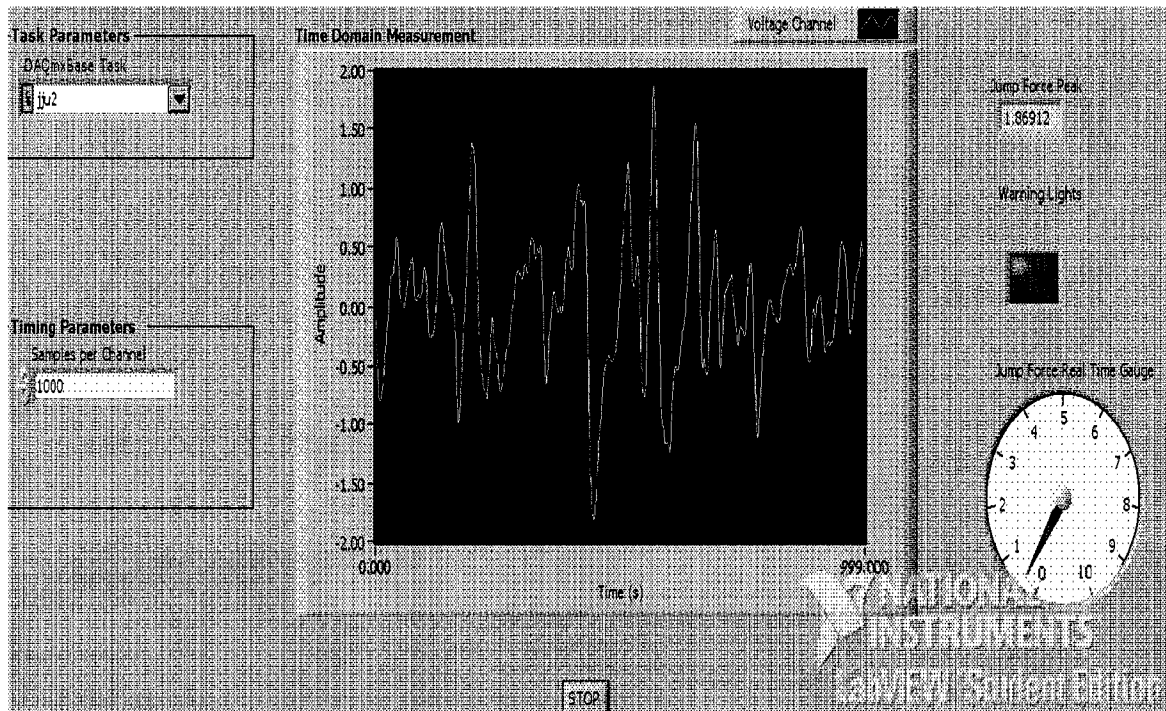
The number “1000” on the left lower corner is the sample size in display window. The user can define the number of samples to be displayed. The top left is the task defined for the input analog signal properties include sampling frequency and

associated input analog ports of USB-6009. The top right window displays the peak value of the real time measurement for the jump force. An alarm LED on the right side will be activated (RED) whenever the signal peak is higher than threshold setup inside the comparator block. The default color for normal LED state is GREEN. The down right side is a virtual gauge to display the jump force in a real-time manner and more intuitively. A “STOP” button at the bottom is used to fully stop the data acquisition process when it is pressed.



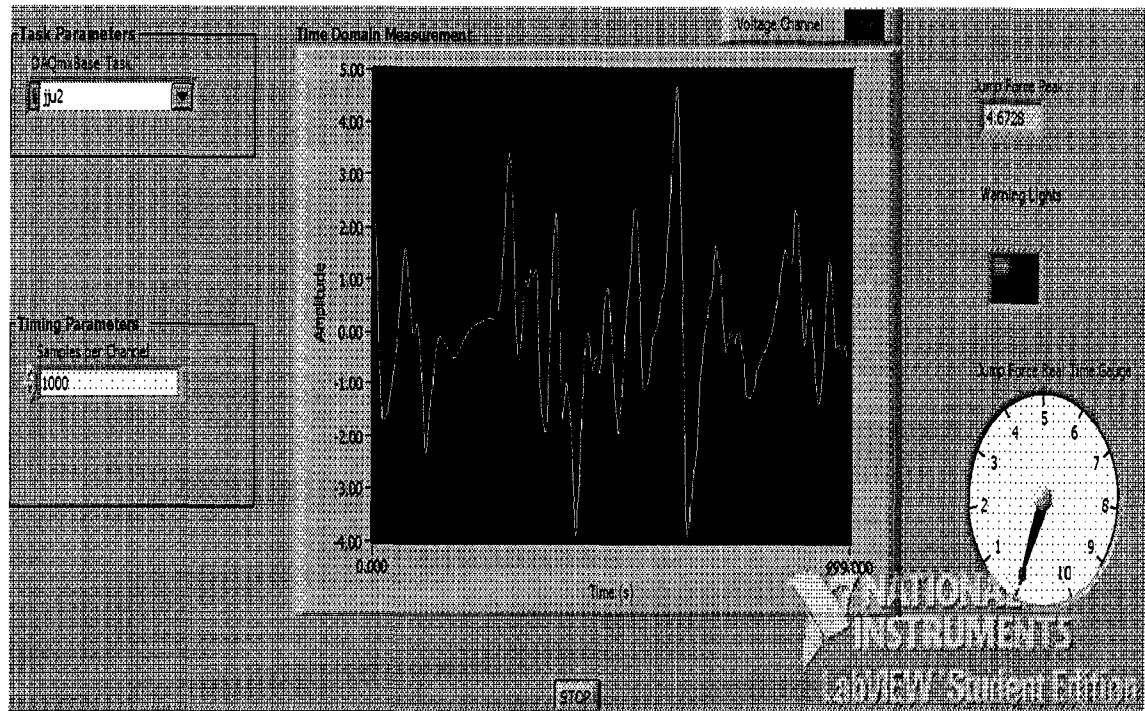
**Figure 3.3a Jump Force Measurements for Position 2 in Figure 3.1**

Figure 3.3a is the measurement of position 2 with peak value of about 337mV due to more strained muscle of position 2 compared with position 1. Both positions stand still without lifting the heels of the feet.



**Figure 3.3b Jump Force Measurements for Position 2  
with Muscles Half Stretched**

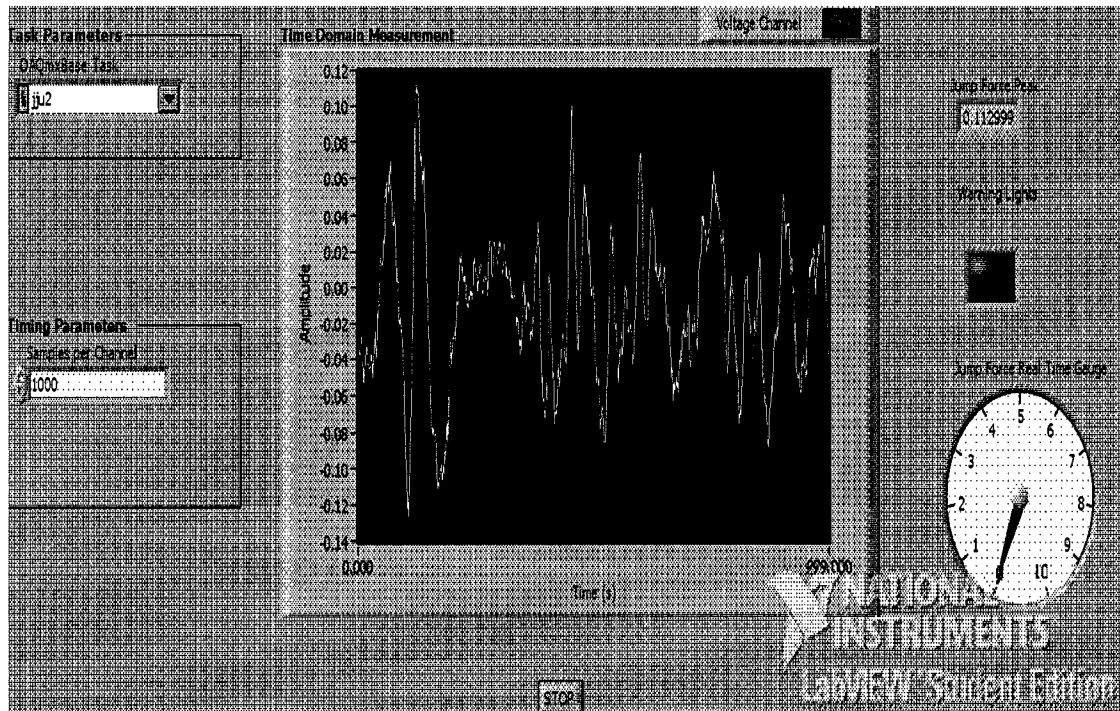
Figure 3.3b is also the measurement of position 2 but with both heels half lifted from ground. This is to simulate the position between fully standing on the toes and position 2 with the feet fully on ground. Peak value of about 1.87V is detected and the alarm LED is still OFF. But the data shows that muscle under half strained case has much higher sensor output than the still standing of the same position 2 in figure 3.1.1.



**Figure 3.3c Jump Force Measurements for Position 2 with Take-Off Jump**

Figure 3.3c is a case to show the jump force value measurement with a forceful jump. The peak value (maximum of the signal) is about 4.67V. The alarm LED is turned ON. The measured jump force is much higher than both the still standing (figure 3.1.3a) and half strained case (figure 3.1.3b).

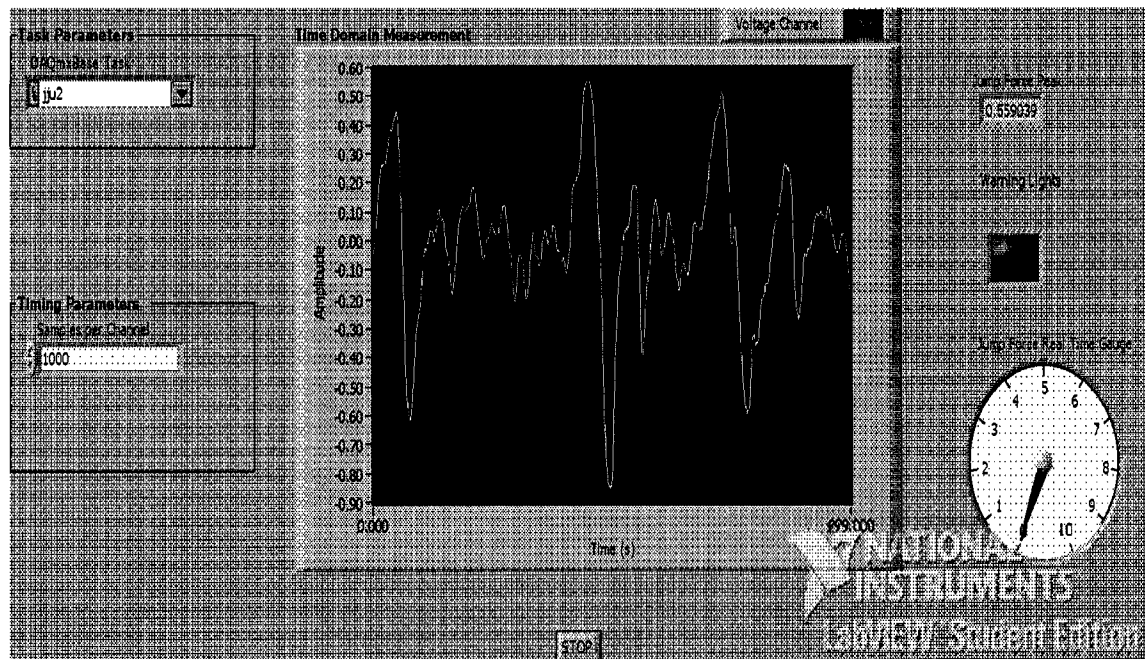




**Figure 3.4 Jump Force Measurement of Third Position in**

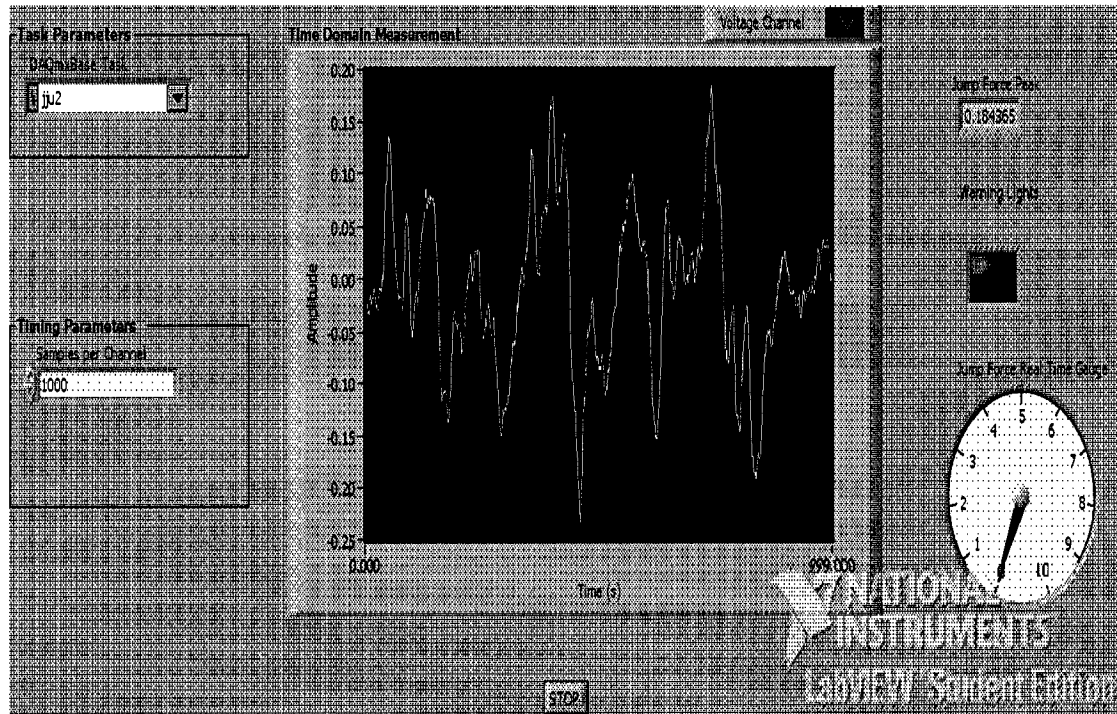
**Figure 3.1**

Figure 3.4 displayed the jump force measurement of position 3 with Peak value of about 113mV, which simulates a still position 3. The alarm LED is OFF.



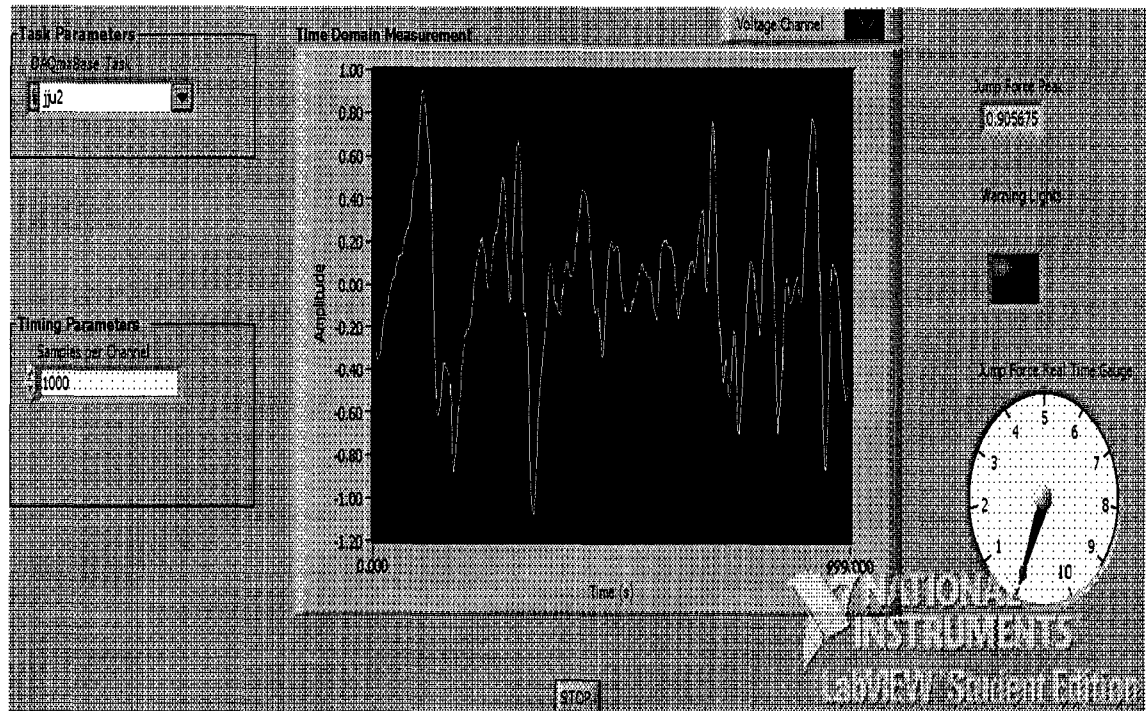
**Figure 3.5 Jump Force Measurement of Fourth Position**

Figure 3.5 is the measurement of jump force of the still position 4. The peak value is about 559mV. The alarm LED is again OFF.



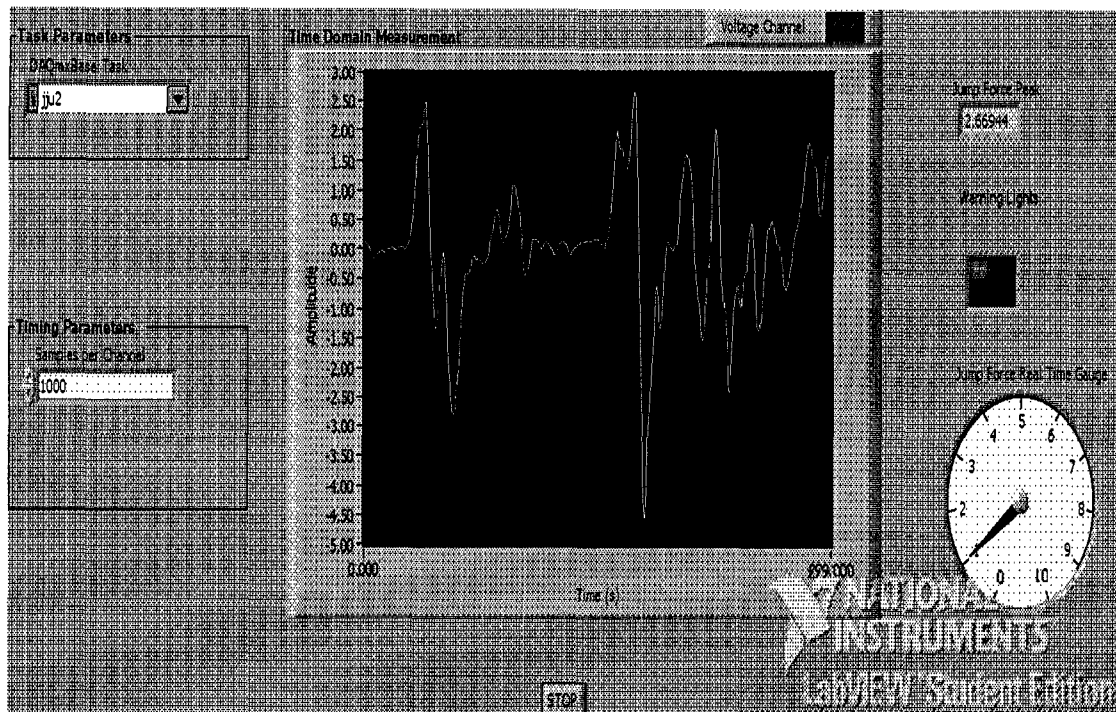
**Figure 3.6a Jump Force Measurement of Relaxed Fifth  
Position**

Figure 3.6a is the measurement of still position 5 with still standing. The peak value is about 184mV. The alarm LED is OFF.



**Figure 3.6b Jump Force Measurement of Fifth Position with  
Muscle Half Stretched**

Figure 3.6b is the measurement of position 5 with muscle half stretched similar to the case described for figure 3.3b. This is to simulate the actions with heels lifted off ground without fully stretched the muscles. The peak value is about 906mV, which is much higher than the still standing of position 5 in figure 3.6a. The alarm LED is still OFF.



**Figure 3.6c Jump Force Measurement of Fifth Position with  
Take-Off Jump**

Figure 3.6c is the data collected to show the full jump based on the position 5. The peak value is about 2.66V, which turns on the alarm LED (2V threshold is set for this experiment). The end users can set up their own alarm threshold based on the statistic studies for specific activities. The peak value with take-off jump is much higher than previous movement in figure 3.6b. It seems that take-off jump usually has the worst strain to the muscles.

## **CHAPTER IV**

### **SUMMARY**

Through the research and design of this system, the knowledge learned through the courses such as active filter design, application circuit design and biomedical instrumentation is practiced.

The purpose of this research is to provide a feasibility studies through the design of a monitoring system based on virtual instrumentations. The system described in this thesis is capable of detecting the primary dancing positions and offers a real-time monitoring. The proposed system design in this thesis can offers friendly human-to-machine interface with real time accurate data acquisition and alarming. The effective gain and filtering/condition circuit is proven to be very effective in both simulation and implementation level.

There is also some weakness in this system mainly in the signal conditioning circuit. More sensitivity studies should be made for both filter and gain stages versus power supply rail fluctuation or each individual capacitor tolerance. By those kinds of detailed studies, further knowledge about the system error or tolerance can be achieved. The alarm threshold needs to be more practical based on repetitive data collection and analysis. In this design, a simple threshold value is used for system feasibility study only

So the system is not ready to be a fully developed instrumentation utilized by business sectors.

## **1 Future Work**

For future further research, some improvement needs to be done to make this system practical for real application.

- i. Adding the micro-processor into the hardware so that a DCS (Distributed Control System) can be implemented. The micro-processor will be programmed with real-time monitoring functions and alarm functions through speakers or hardware LED when the jump force is more than the threshold.
- ii. The UART interface of the processor above can be converted to USB interface via the UART-to-USB bridge controllers. New technology such as Wireless USB interface is desirable so that the sampled data can be transmitted to the remote PC or notebook without physical cable, which makes the device convenient to carry for performers. The virtual instrumentation in computers can receive the data and perform the statistic analysis based on daily activities or monthly activities. The PC here acts as the central control of the DCS system. The user can store the data to hard disk or removable device for diagnosis purpose if applicable.
- iii. Software program improvement with the addition of expert system is desirable. With the data collected through Wireless USB interface and the statistics analysis, some advice can be made to the dancer via the rule-based expert system.

iv. Alarming threshold of jump force in this design may depend on the position of electrode, the muscles locations and ages of ballet performer. More studies in the future are needed including a better human-to-machine graphics interface to allow the user to set up the different threshold for different dancers. Software may help the dancer to determine a suitable threshold based on the daily statistics of the measurement data. Thus the system will be an even more effective and interactive device for dancers to monitor the electromyographic activity.



## LIST OF REFERENCES

1. Nevenka Kozomora, "Using the FSR in Biometrics Measurement" Independent Study, Instructor: John LaCourse, Chairman and Professor of University of New Hampshire, 2003.
2. [www.bbc.co.uk/music/dancersbody/body/jumping.shtml](http://www.bbc.co.uk/music/dancersbody/body/jumping.shtml).
3. Jeffrey R. Cram, PhD, Glenn S.Kasman, ,Jonathan Holtz,,,"Introduction to Surface Electromyography",1998, pp.43-51 and pp373-374.
4. Steven Christopher Koenig, "Analysis of Human Functional Mobility Via The Actimeter", MSEE Thesis, University of New Hampshire, 1990.
5. William D. Stanley ,Old Dominion University ,,"Operation Amplifiers with Linear Integrated Circuits" Second Edition, 1994, PP104-112,PP182-189, PP348-368.
6. John G. Webster, "Medical Instrumentation Application and Design", Third Edition, PP259-260.